Paleoproterozoic Bonnet Plume River intrusions: Evidence for a calc-alkaline arc at 1.7 Ga and its partial preservation in Yukon, Canada

Alexander B. Nielsen[1], Derek J. Thorkelson, Daniel D. Marshall and H. Daniel Gibson
Department of Earth Sciences, Simon Fraser University

Nielsen, A.B., Thorkelson, D.J., Marshall, D.D. and Gibson, H.D., 2011. Paleoproterozoic Bonnet Plume River intrusions: Evidence for a calc-alkaline arc at 1.7 Ga and its partial preservation in Yukon, Canada. *In:* Yukon Exploration and Geology 2010, K.E. MacFarlane, L.H. Weston and C. Relf (eds.), Yukon Geological Survey, p. 183-196.

ABSTRACT

The 1.71 Ga Bonnet Plume River intrusions (BPRI) and related volcanics are preserved only as clasts in the 1.60 Ga Wernecke breccias of Yukon that host iron-oxide copper gold (IOCG) occurrences. Field work conducted in 2009 confirmed that they did not intrude the surrounding <1.64 Ga Wernecke Supergroup. Petrography shows that they are extensively altered and/or metasomatized, although relicts of primary igneous minerals remain. The major oxides are of little use in classification. Trace element geochemistry however, reveals a mafic to intermediate, calc-alkaline volcanic arc signature. Geochemical modelling has demonstrated that crystal fractionation was dominated by pyroxenes, plagioclase and olivine. The BPRI and related volcanic rocks are thought to have originated in a calc-alkaline volcanic arc that was obducted onto the Wernecke Supergroup, subsequently partially brecciated, and finally sank within the Wernecke breccias to the level of the Wernecke Supergroup.

[1]onielsen@sfu.ca

INTRODUCTION

LOCATION, ACCESS AND METHODS

Fieldwork in 2009 was undertaken in order to investigate and sample the Bonnet Plume River intrusions (BPRI) and other igneous rocks at known mineral occurrences across the Yukon (Fig. 1). With the exception of 'Spectacular Creek' (Yukon Olympic MINFILE occurrence 116G/082), all locations are remote and accessible only by helicopter. The Spectacular Creek location is most easily accessed by crossing the Blackstone River by small watercraft. BPRI exposures were examined at each of the field locations (investigation sites, Fig. 1). Volcanic and plutonic rocks correlated with the BPRI were examined at the Spectacular Creek locality. At two locations, near the Bel and Pika MINFILE occurrences, detailed maps were made to show the relationship between the igneous clasts and the surrounding breccias (Figs. 2 and 3).

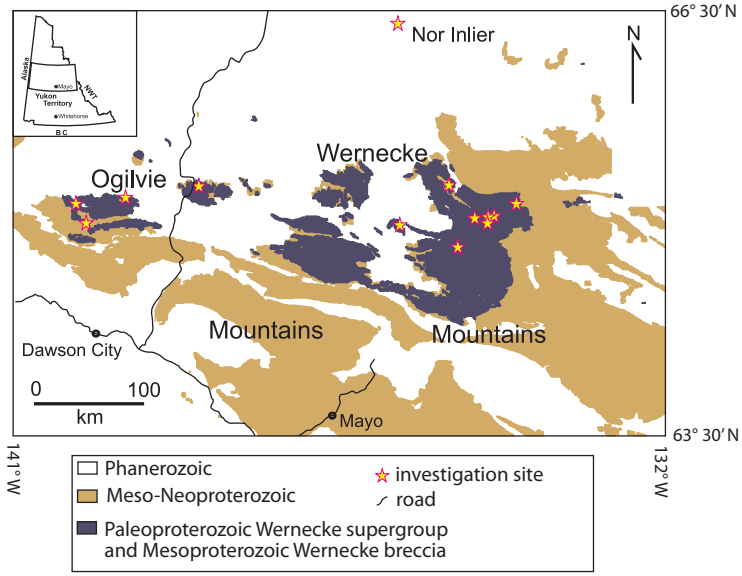

Figure 1. *Map of central Yukon illustrating the distribution of Proterozoic inliers and locations where field work was conducted.*

REGIONAL GEOLOGY

The Paleoproterozoic (1725 -1705 Ma) BPRI comprise bodies of metamorphosed diorite, gabbro, basalt and andesite, as well as minor anorthosite and quartz-albite syenite (Thorkelson *et al.*, 2001a). Diorite clasts are most common. These bodies of igneous rock are present only as clasts within the Mesoproterozoic Wernecke breccia systems (1595 Ma; Thorkelson *et al.* 2001b). Unbrecciated examples of the Bonnet Plume River intrusions are not known.

Zones of Wernecke breccia are exposed in Proterozoic inliers in the Wernecke, Ogilvie and Richardson mountains throughout the central and northern Yukon (Fig.1). They intrude the Mesoproterozoic (minimum age 1595 Ma, maximum age 1640 Ma; Thorkelson *et al.,* 2001b; Furlanetto *et al.*, 2009a) Wernecke Supergroup (Fig.1), a 13 to 14 km-thick sedimentary succession (Delaney, 1981; Norris, 1997; Thorkelson, 2000). Prior to brecciation, the Wernecke Supergroup was deformed and locally metamorphosed to middle-upper greenschist grade during the Racklan orogeny (Thorkelson *et al.,* 2000; Brideau *et al.*, 2002). The Wernecke breccias and the BPRI host numerous iron-oxide copper gold (IOCG) occurrences (Thorkelson, 2000).

PREVIOUS WORK

The remote locations and difficult access has meant that the BPRI have received only cursory investigation in the past. The first major study was conducted by Thorkelson (2000), and was expanded upon in Thorkelson *et al.* (2001a,b), following regional mapping by Thorkelson and Wallace (1998a,b,c) in the Wernecke Mountains. Key results include that the BPRI crystallized between 1725 Ma and 1705 Ma, and that the crystallization preceded their inclusion in the Wernecke breccias.

Laughton *et al.* (2002) studied the Slab volcanics, which comprise a series of mafic volcanic clasts, including a megaclast at Slab Mountain consisting of 35 amygdaloidal basaltic pahoehoe flows. Laughton *et al.* (2002) concluded that they are probably correlative with the BPRI. Following this, Hunt and Thorkelson (2007) studied mafic igneous rocks in the Wernecke breccias in the eastern Ogilvie Mountains and Nor inlier (Fig. 1). On the basis of field relationships, and major and trace element geochemistry, it was determined that these rocks are probably correlative with the BPRI.

WHY REINTERPRET THE ORIGINS OF THE BPRI?

A previous model of geological events described the BPRI as igneous intrusions hosted by the Wernecke Supergroup (Thorkelson, 2000; Thorkelson *et al.*, 2001a,b), with both intrusions and host affected by hydrothermal activity and formation of Wernecke breccia. However, a detrital mineral study by (Furlanetto *et al.*, 2009a) indicated that the Wernecke Supergroup is <~1640 Ma, which is ~75 m.y. younger than the BPRI. This age difference indicates that the BPRI could not have intruded the Wernecke Supergroup, and that a different explanation is required to account for the presence of the BPRI in the Wernecke breccias.

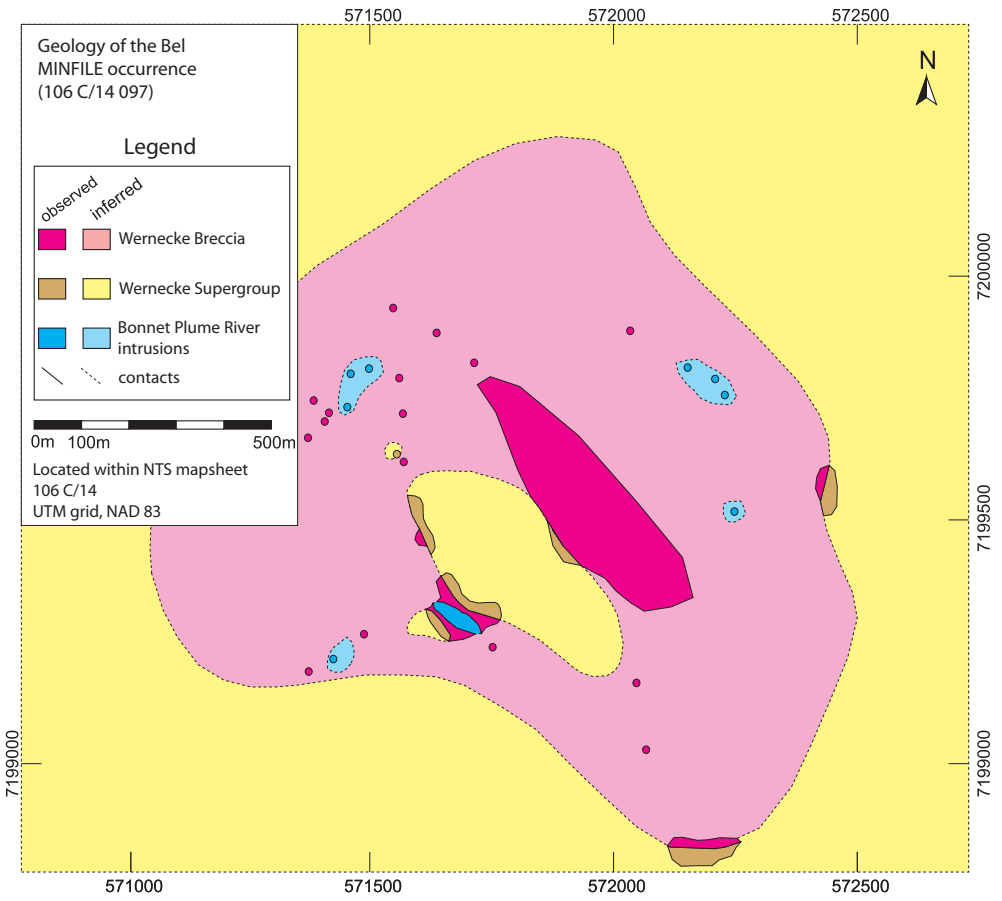

Figure 2. *Geological map of the Bel MINFILE occurrence (106C/14 097).*

FIELD RELATIONSHIPS

The BPRI are the oldest known rocks in the Yukon at 1710 Ma (Thorkelson *et al.,* 2001a). They exist only as clasts within the Wernecke breccias. Thorkelson *et al.* (2001a) proposed that there are BPRI bodies with igneous contact relationships with the Wernecke Supergroup; however, the age relationship between the BPRI (1710 Ma) (Thorkelson *et al.*, 2001a) and the Wernecke Supergroup (maximum 1640 Ma, Furlanetto *et al.*, (2009a)) casts doubt on this relationship. More detailed work during the 2009 field season was carried out at many of the locations where igneous contact relationships between the BPRI and Wernecke Supergroup were inferred in the original mapping by Thorkelson and Wallace (*e.g.*, 1998a,b,c). In all cases, the BPRI were not in igneous contact with the Wernecke Supergroup; they were separated by a zone of Wernecke breccia. This separation was commonly on the order of 1-10 m (Figs. 2 and 3). Furthermore, the BPRI do not show grain size variations consistent with chilling along their margins, and the Wernecke breccias are not contact-metamorphosed by the BPRI. This understanding is consistent with the isotopic age of the Wernecke breccias (~1595 Ma; Thorkelson, 2000), which is ~115 Ma younger than the BPRI.

Clasts of BPRI are up to 900 m long and 200 m wide. The BPRI are not metamorphosed above middle greenschist grade. The Wernecke breccias lack any clasts which would suggest derivation from a basement source under the Wernecke Supergroup such as gneiss and peridotite.

PRIMARY AND SECONDARY MINERALOGY

The mineralogy of the BPRI reflects both primary (igneous) and secondary (metasomatic and metamorphic) mineral growth. The observed mineral assemblage of the Bonnet Plume River intrusions may be divided into three groups: primary igneous minerals; secondary minerals that are pseudomorphs of the primary minerals; and secondary minerals that occur in veins, mats and mineral overgrowths (Table 1).

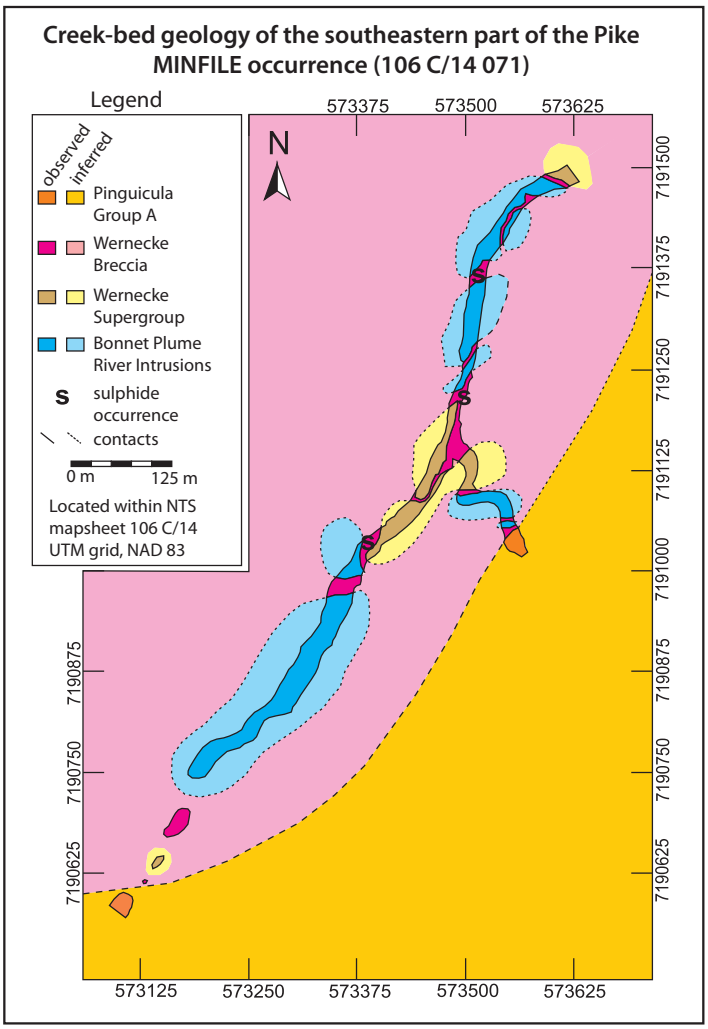

Figure 3. *Geological map of part of the Pika MINFILE occurrence (106C14 071).*

The inferred primary mineralogy of the BPRI, without metasomatic minerals, consists of pyroxenes, plagioclase and olivine, as well as rare quartz and potassium feldspar. Based on the quartz-alkali feldspar-plagioclase-feldspathoid classification system of LeMaitre (2002), the BPRI are primarily diorites and gabbros with minor quartz diorite, tonalite, granodiorite and quartz monzodiorite.

The mineralogy of the BPRI is dominated by secondary minerals, primarily chlorite, epidote, sericite, Na-Ca zeolites and iron oxides. Potassium feldspar is commonin more potassically altered samples. Veins in the BPRI are composed primarily of calcite, commonly with quartz and other minor phases.

Sericite, scapolite and Na-Ca zeolites form partial to complete replacements of plagioclase (Fig 4a). Chlorite is present as pseudomorphs of euhedral phenocrysts (former pyroxene or olivine crystals) in fine-grained BPRI, or as well defined zones bounded by plagioclase pseudomorphs (Fig. 4b), and also in groundmass and undefined parts of the rock. Commonly, the chlorite pseudomorphs include grains of hematite. Hematite also forms pseudomorphs of magnetite and possibly ilmenite, as well as newly formed metasomatic porphyroblasts (Fig. 4c). These relationships are summarized in Table 2.

Table 1. *Occurrence of minerals observed in thin section. Dots indicate known occurrence; question marks indicate uncertain presence.*

Mineral	Occurs as a primary mineral	Occurs as a pseudomorph	Occurs as overgrowths	Occurs in veins
plagioclase	*			*
alkali feldspar	*	*		
Na-Ca zeolites		*		
muscovite (sericite)		*		
hornblende		*		
chlorite		*	*	*
scapolite		*		
epidote			*	*
biotite			*	
calcite			*	*
quartz	*			*
apatite				*
hematite		*	*	
magnetite	?		*	
pyrite	?		*	
chalcopyrite			*	

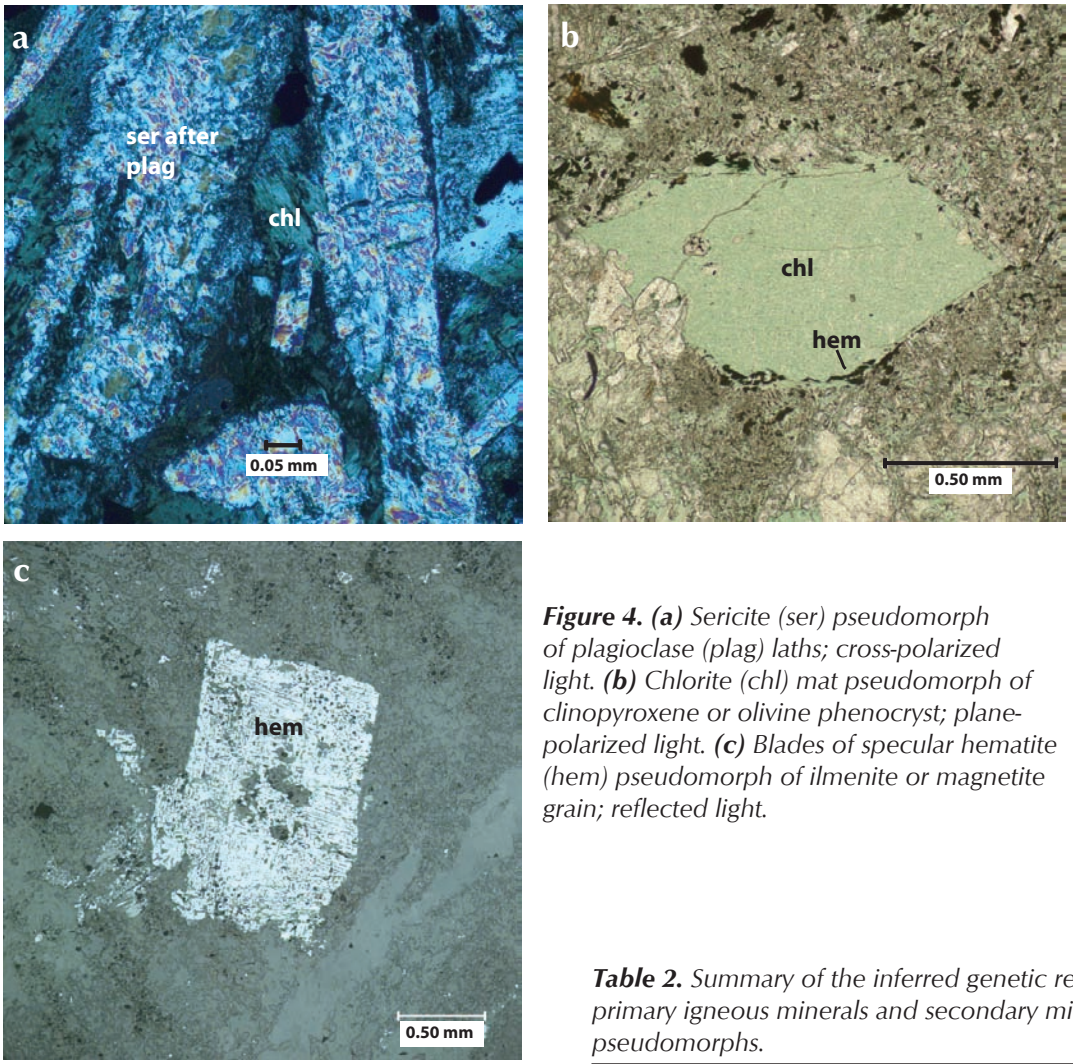

Figure 4. ***(a)*** *Sericite (ser) pseudomorph of plagioclase (plag) laths; cross-polarized light.* ***(b)*** *Chlorite (chl) mat pseudomorph of clinopyroxene or olivine phenocryst; plane-polarized light.* ***(c)*** *Blades of specular hematite (hem) pseudomorph of ilmenite or magnetite grain; reflected light.*

Table 2. *Summary of the inferred genetic relationships between primary igneous minerals and secondary minerals that are present as pseudomorphs.*

Primary minerals	Secondary minerals
igneous crystallization	metamorphism and metasomatism
plagioclase	Na-Ca zeolites sericite scapolite alkali feldspar
olivine pyroxene amphibole	chlorite
magnetite ilmenite	hematite

GEOCHEMISTRY

Thirty samples of BPRI were analysed for major and trace elements at Activation Laboratories in Ancaster, Ontario, and the resulting data have been added to previously collected data for the BPRI from Thorkelson (2000) and unpublished data from the Slab volcanics (Laughton, 2004) in order to create a more robust data set.

MAJOR ELEMENT COMPOSITIONS

Silica concentrations for BPRI cluster in the range of 45-55% and a few samples to almost 70% (Fig. 5). When plotted against hafnium (Hf) (Fig. 5), a relatively immobile element, most major oxides display a high degree of scatter, particularly those that are mobile in hydrothermal solution such as the alkalis and alkaline earths. In contrast, alumina forms a relatively tight linear array. Given that alumina is relatively immobile in hydrothermal conditions, much of the scatter of the other oxides is probably the result of metasomatic alteration rather than igneous processes such as fractional crystallization. The main cause of the hydrothermal alteration is probably fluid activity during Wernecke breccia formation, which is widely recognized in wallrock and clasts of Wernecke breccia (Thorkelson *et al.*, 2001b).

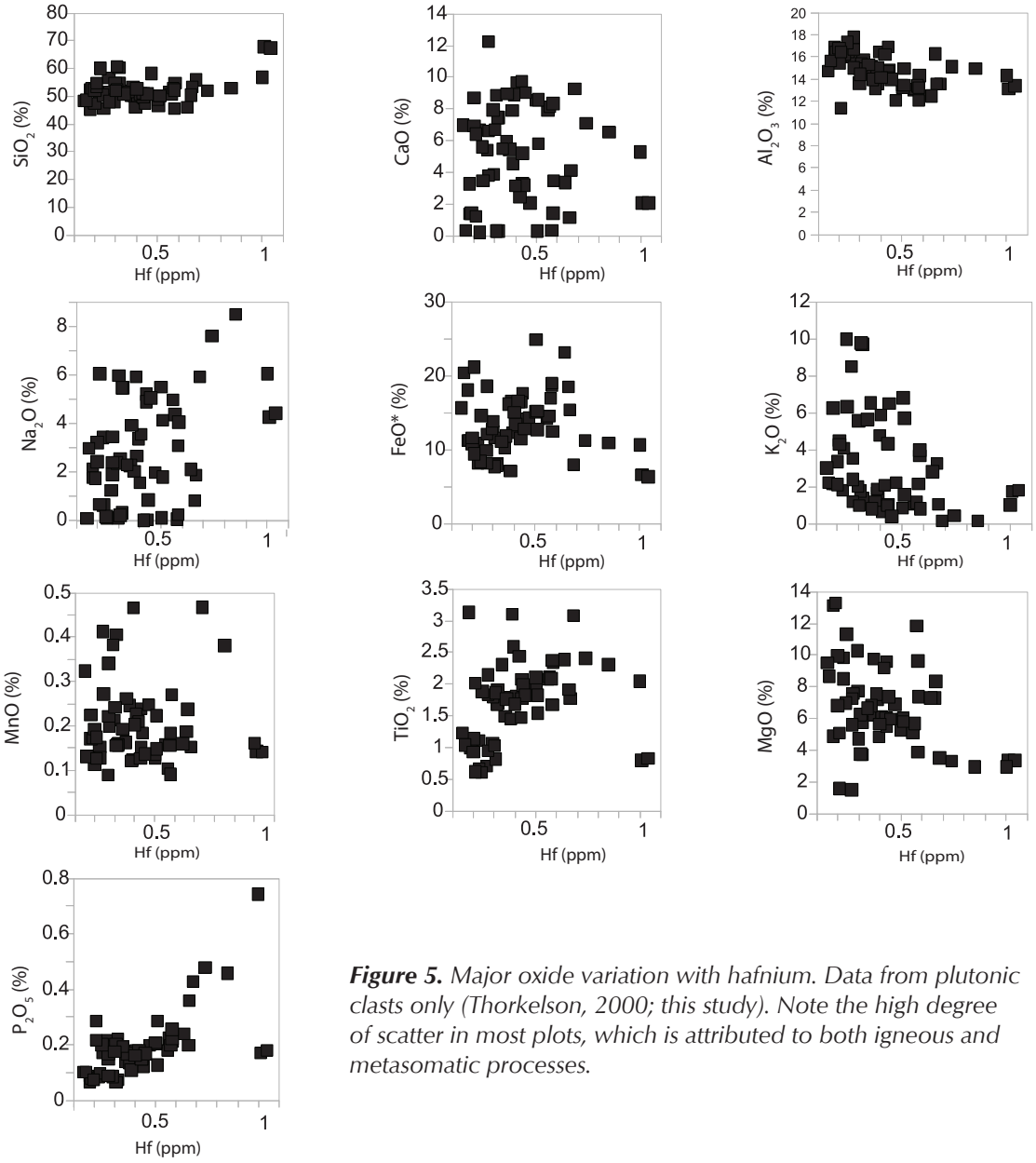

Figure 5. *Major oxide variation with hafnium. Data from plutonic clasts only (Thorkelson, 2000; this study). Note the high degree of scatter in most plots, which is attributed to both igneous and metasomatic processes.*

The CIPW normative mineralogy of the BPRI is highly variable, largely due to major element mobility. Samples range from 22% quartz to 15% nepheline and 6% leucite in their normative mineralogies. Plagioclase compositions range from An_0 to An_{96}. Whole-rock Mg numbers range from 29 to 69. Samples are peraluminous to metaluminous. These compositional variations likely reflect the original igneous compositions with significant modifications from brecciating fluids.

CALC-ALKALINE DIORITES AND GABBROS

DIFFICULTIES IN GEOCHEMICAL DISCRIMINATION OF THE BPRI AND RELATED VOLCANICS

Systems of classifying, determining rock series, and assigning tectonic affinity of rocks are commonly based on major elements and/or mobile trace elements. These elements do not generally retain their primary concentrations after metasomatism by hydrothermal fluids; therefore, systems based on these concentrations are likely to produce results with a wide and meaningless scatter. In order to address this issue, systems based on immobile elements have been applied to the BPRI (Floyd and Winchester, 1978; Rollinson, 1993; Gifkins *et al.,* 2005).

ROCK CLASSIFICATION

The system of Winchester and Floyd (1977) has been used for classifying the BPRI. In this system, the BPRI are predominantly subalkaline basalt and andesite, and minor rhyodacite-dacite, rhyolite, trachyandesite and alkali basalt (Fig. 6). Given that many of the BPRI are phaneritic, plutonic rock names of comparable composition are generally more appropriate. Accordingly, the BPRI should be regarded as mostly diorite and gabbro, and minor granodiorite, tonalite and quartz monzonite.

The commonly used TAS method of Le Maitre (2002) was not used due to the open-system behaviour of the alkalis and to a lesser degree, silica, in the BPRI. When the TAS system is applied, it produces an extremely wide array of rock types, with samples plotting evenly among the basalt to trachydacite fields, in all three levels of silica saturation.

ROCK SERIES

In order to further describe the composition of the BPRI, the method of Ross and Bédard (2009) was applied. This method demonstrates that the BPRI follow the calc-alkaline to transitional series trend, as opposed to a tholeiitic one (Fig. 7). This differentiation method is more robust than the standard methods of differentiating the magma series of rocks (*e.g.*, Irvine and Baragar, 1971; Miyashiro, 1974; Pecerillo and Taylor, 1976) because it is based on the ratios of relatively immobile trace elements.

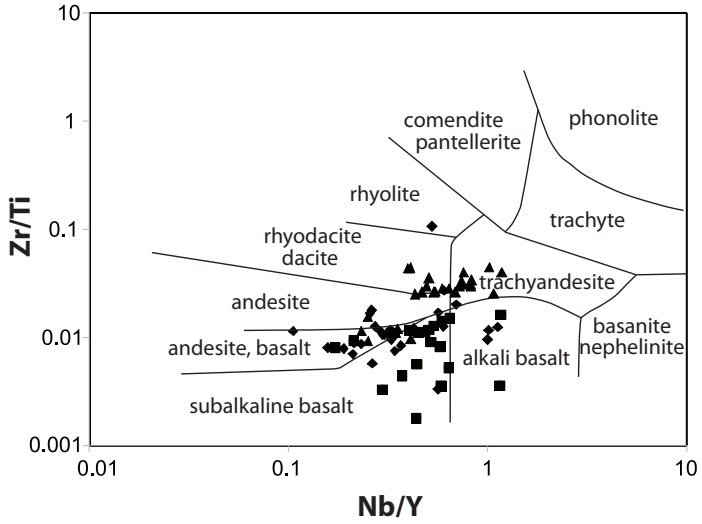

Figure 6. *Rock classification after Winchester and Floyd (1977). Diamonds indicate data from this study, squares indicate data from Thorkelson (2000), and triangles indicate data from Laughton et al. (2002).*

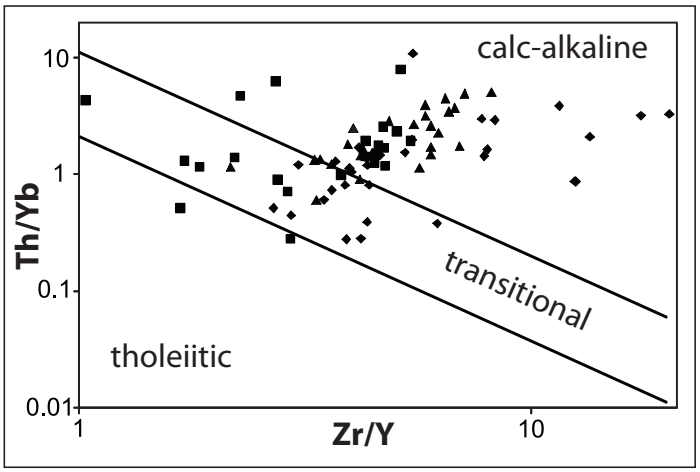

Figure 7. *Rock series classification after Ross and Bédard (2009); logarithmic scale. Diamonds indicate data from this study, squares indicate data from Thorkelson et al. (2001a), and triangles indicate data from Laughton et al. (2002).*

ARC AFFINITY OF THE BPRI

An N-MORB-normalized spider diagram including the BPRI and related volcanics is illustrated in Figure 8 (normalizing values Cs-Lu after Sun and McDonough, 1989; Gd-Ti order reversed after Pearce and Parkinson, 1993; Co to Ni after Pearce and Parkinson, 1993, except Zn and Cu, estimated

by D.J. Thorkelson (unpublished data), and from Basaltic Volcanism Study Group, 1981). The strongly enriched large-ion lithophile elements, relative Nb-Ta depletion, and gently right-sloping rare-earth element pattern that approaches unity, indicate that the BPRI probably formed in an arc to back-arc setting. The scatter on the diagram may reflect fluid-induced remobilization, but the general shape of the pattern reflects original igneous compositions.

ARC AFFINITY REVEALED BY IMMOBILE ELEMENTS

Thorkelson *et al.* (2001a) attempted to characterize the tectonic affinity of the BPRI based on the Ti/V ratio of Shervais (1982) and the La/Th, La/Ba and Nb/La ratios of Gill (1981). This attempt was inconclusive because Ba and Ti have a large scatter, probably due to metasomatism during the emplacement of the Wernecke breccias. Immobile element (Th, Nb, La, Hf, Ta and Yb) ratio plots of the BPRI and associated lavas demonstrate a strong geochemical similarity to calc-alkaline arcs (Figs. 9 and 10; Wood, 1980; Gill, 1981).

GEOCHEMICAL MODELLING

Geochemical modelling was performed on the BPRI in order to investigate whether their major and trace element characteristics can be explained by closed-system Rayleigh fractionation and if metasomatic processes could be recognized. This was done with (1) a numerical model of major element trends-based mineral compositions, and (2) models of mineral-specific partition coefficients for the trace elements. The modelling demonstrated that the geochemical patterns of the BPRI can be explained by Rayleigh fractionation, and that metasomatism and other open-system processes, such as crustal assimilation and mixing, play a significant role.

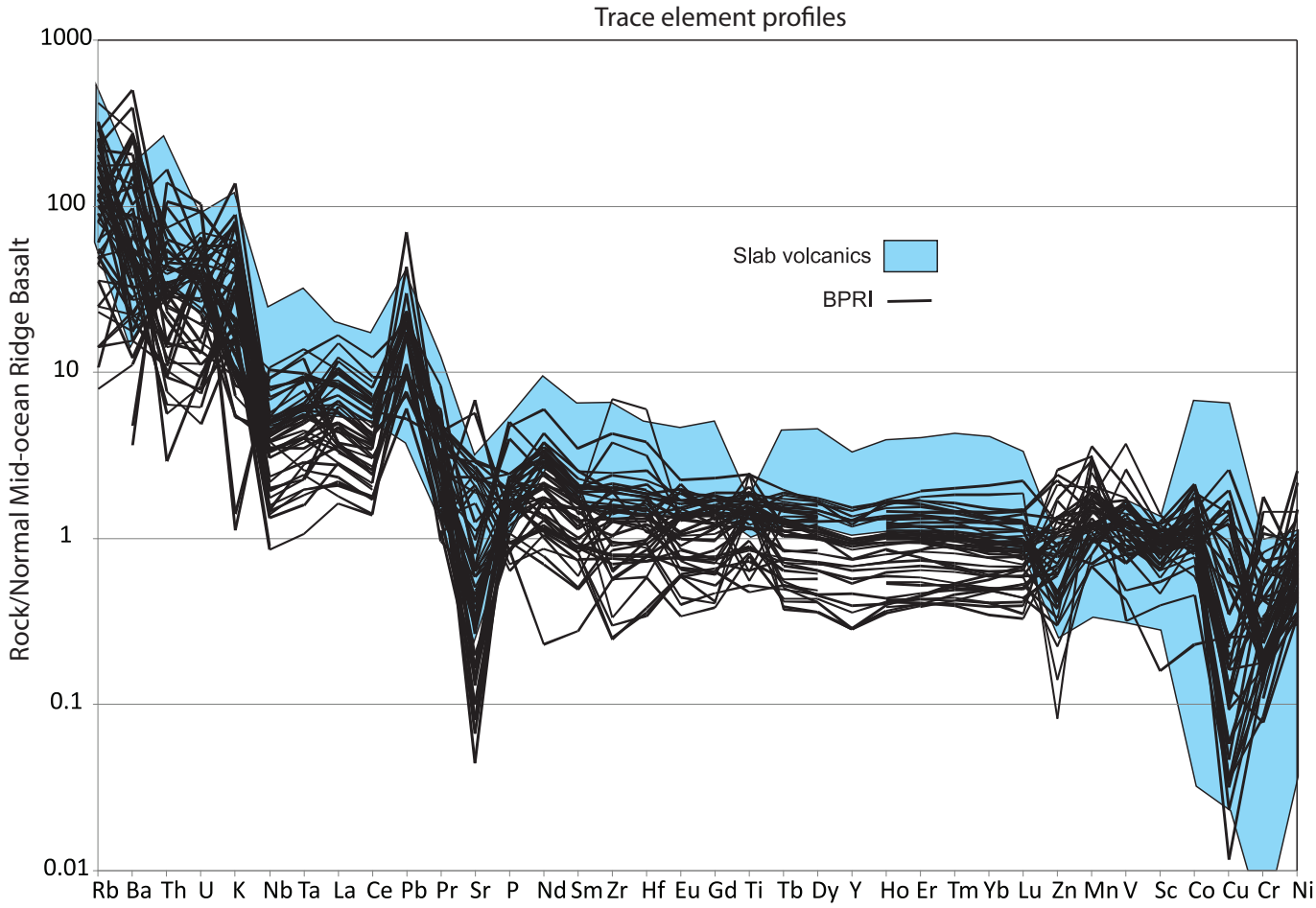

Figure 8. *N-MORB normalized (normalizing values Cs-Lu after Sun and McDonough (1989); Gd-Ti order reversed after Pearce and Parkinson (1993); Co to Ni after Pearce and Parkinson (1993) except Zn and Cu, estimated by D.J. Thorkelson (unpublished data) and from Basaltic Volcanism Study Group (1981)) spider diagram illustrating data from this study and Thorkelson et al., (2001a; black lines), and the Slab volcanics (light blue field).*

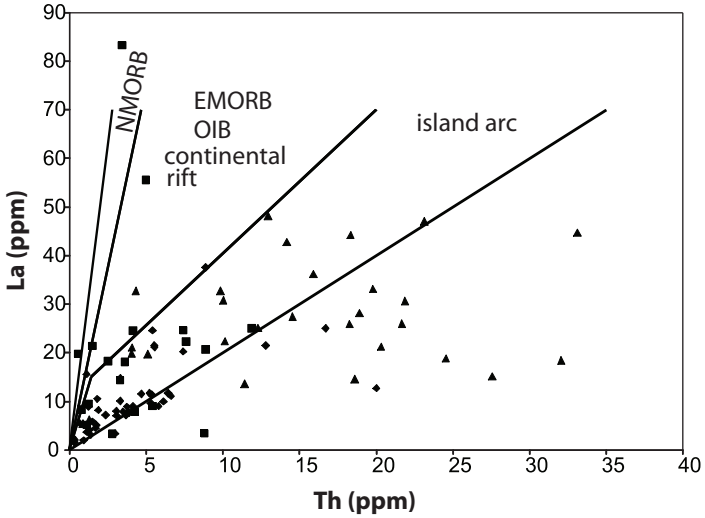

Figure 9. *Tectonic affinity plot, modified after Gill (1981), based on La and Th. Samples plot predominantly in the arc volcanics field. Diamonds indicate data from this study, squares indicate data from Thorkelson et al. (2001a), and triangles indicate data from Laughton et al. (2002).*

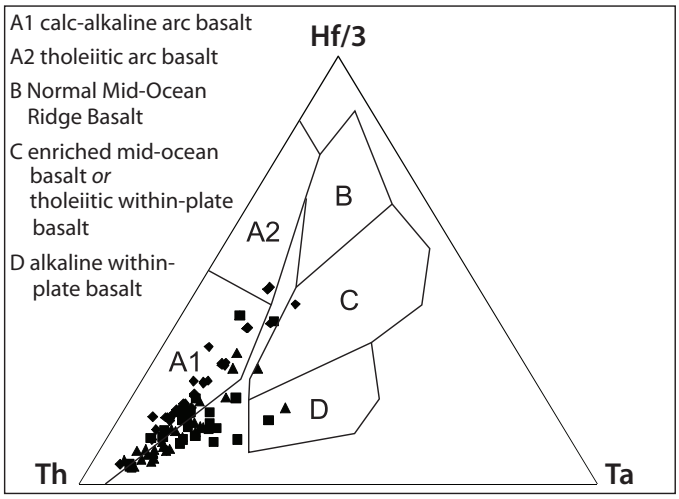

Figure 10. *Tectonic affinity plot, after Wood (1980), based on Hf, Th and Ta. Samples plot predominantly in the calc-alkaline arc basalt field. Diamonds indicate data from this study, squares indicate data from Thorkelson (2000), and triangles indicate data from Laughton et al. (2002).*

METHODS

Major element geochemical modelling is preliminary and reflects a first attempt to model rock evolution using two of the least metasomatized samples of BPRI, as determined petrographically. One sample had high levels of Mg, Cr, Ni and Sc and was therefore regarded as a possible parent to other BPRI units. The other had lower levels of these elements and a high level of potassium. Zr was used as a conserved element against which igneous and open-system processes were gauged. The parental composition plots as a horizontal line and has a value of 1; geochemical losses and gains relative to variations in Zr plot below and above the parental composition in Figure 11, respectively. Elemental losses from the primary composition were modelled by removal of stoichiometrically appropriate molar quantities of major elements based on the compositions of minerals that were hypothesized to have crystallized and subsequently removed from the magma system (except for Na which could only be modeled by metasomatic and igneous depletion). Elemental gains were modelled using individual elements without stoichiometric constraints. This procedure was deemed to be the most suitable approach because there is no necessity for metasomatic processes to add or remove mineralogically defined molar quantities of elements.

The trace element modelling used all available data for the BPRI. Differentiation trends were defined by ratios of trace element partition coefficients into olivine, orthopyroxene, clinopyroxene, plagioclase, and hornblende, plotted as fractionation vectors in Figure 12. A model differentiation trend was defined using an appropriate weighted average of the differentiation trends of these minerals. This trend was defined visually in order to approximate the distribution of data points. The mineral proportions defining this trend reflect the relative abundances of dominant phases that fractionated during the evolution of the BPRI.

IGNEOUS AND METASOMATIC PROCESSES

Major element modeling indicates that geochemical variations were produced mainly by augite, orthopyroxene and plagioclase fractionation, and only minor removal of magnetite, rutile, titanite and apatite (Fig. 11). The total amount of fractionation was nearly 50%. However, despite using the least altered samples in the major element modelling, it was necessary to invoke open-system processes such as metasomatism, crustal assimilation, or variable primary magma systems in order to model the calculated bulk composition differentiation trend. Specifically, concentrations of K_2O, Na_2O, TiO_2 and P_2O_5 could not be modelled by mineral fractionation alone, and required elemental additions or subtractions. The alkali elements showed the greatest divergence from closed-system processes, and the high level of potassium in the rock was modeled with an open-system gain of 3.33 mol%, and Na_2O modeled with a loss of 2.6 mol% (Fig. 11). Most of the open-system variability was probably caused by breccia fluid activity.

Trace element geochemical modelling indicates a similar suite of fractionating minerals and range of fractionation percentages. The full range of fractionation was greater than 90%. Across various trace element systems, the minerals that consistently define the model trend were orthopyroxene, clinopyroxene, olivine and plagioclase (Yb-Nb illustrated in Fig. 12). Metasomatism, crustal assimilation, and differences in primary magmas may explain the large range of trace element compositions, because the full range cannot be explained by fractional crystallization alone.

IGNEOUS AND TECTONIC HISTORY

Wernecke breccias, and the clasts contained within, have been the subject of considerable debate, and various models have been proposed including mud diapirs, salt diapirs, epiclastic deposits, diatremes and hydrothermal breccias (see reviews in Thorkelson, 2000 and Thorkelson *et al.*, 2001b). Recent advances in understanding have occurred through the acquisition of new field and analytical data, which confirm that the breccia system was generated by hydrothermal processes but require revisions to regional models of tectonic, magmatic and hydrothermal activity. New information about the BPRI provides constraints on an emerging model of the Paleo-Mesoproterozoic history of the northwestern margin of ancestral North America (present coordinates; Furlanetto, *et al.*, 2009b).

Any model that attempts to explain the assemblage of Paleo-Mesoproterozoic units in the study area should take into account the following key points: (1) field relationships indicate that the BPRI did not intrude the Wernecke Supergroup or Wernecke breccia; (2) the BPRI are located entirely within zones of Wernecke breccia; (3) Wernecke breccia zones are noted within all stratigraphic units of the Wernecke Supergroup; (4) Wernecke breccia formed after Racklan deformation and metamorphism; (5) the BPRI crystallized ~75 Ma before the onset of Wernecke Supergroup deposition, and ~115 Ma before Wernecke breccia formation at 1595 Ma; (6) the geochemical compositions of the BPRI, the Slab volcanics, and other volcanic clasts in Wernecke breccia indicate formation in a calc-alkaline volcanic arc

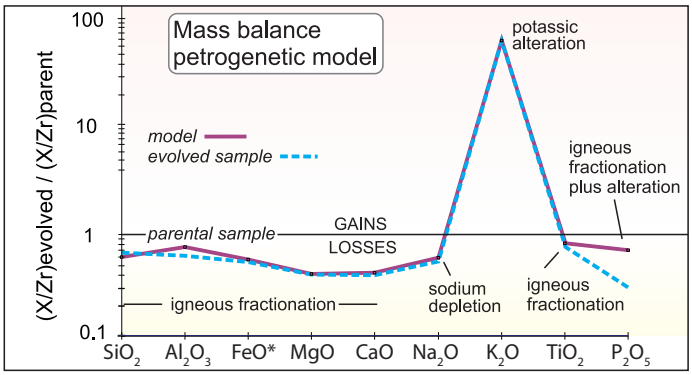

Fractionation phases	Mineral compositons	Percent of phase
plagioclase	anorthite in plagioclase = 60	14.9
augite	diopside in augite = 61	43.6
orthopyroxene	enstatite in orthopyroxene = 61	35.8
magnetite	TiO_2 in magnetite = 15	3.0
rutile		0.9
titanite		0.1
apatite		1.8
Percentage of fractionation		48

Metasomatic gains and losses		Percent of component
Fe_2O_3		0.33
K_2O		3.33
Na_2O	(loss)	-2.66

Figure 11. *Stonergram using mass balance and conserved element logic (using Zr) to model igneous and metasomatic processes between a sample that is inferred to be of parental composition (having high Mg, Sc, Cr and Ni), and a sample that is evolved. Tables summarize the model fractionation assemblage and components added or removed by metasomatizing fluids.*

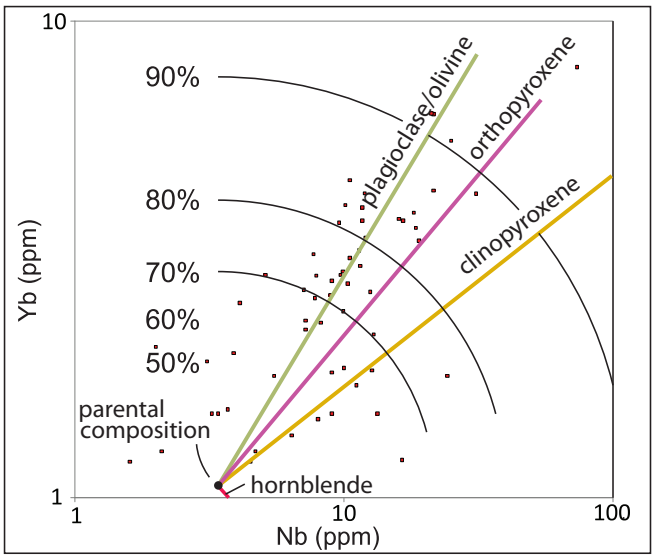

Figure 12. *Distribution of incompatible elements (Nb and Yb) in relation to Rayleigh fractionation vectors. Lines illustrate the fractionation trend away from the same inferred parental sample as in Figure 11. Arcs depict approximate percentage of fractionation.*

(see Peters and Thorkelson (this volume) for additional information); (7) no gneiss or peridotite clasts have been reported from Wernecke breccia; and (8) clasts of the BPRI are up to 900 m in length, and 200 m in width.

The BPRI were not emplaced as magma into either the Wernecke Supergroup, or the Wernecke breccias. They must have been present either above, or below the Wernecke Supergroup at the time of Wernecke breccia formation. Clasts of the BPRI would have been enclosed by Wernecke breccia and transported either upward or downward, and some clasts may have become cemented within zones of breccia at the level of the Wernecke Supergroup. Transport of the BPRI from beneath the Wernecke Supergroup would require upward translation of clasts through nearly the entire succession, *i.e.*, nearly 13 km. This scenario is problematic because it would require hydrothermal solutions to upwardly drive megaclasts which approach 1 km in length. It is also unappealing because clasts of the BPRI are not accompanied by clasts of other rock types that might be situated beneath the Wernecke Supergroup, such as peridotite and high-grade schist and gneiss.

Derivation of BPRI clasts from above the Wernecke Supergroup is more plausible because it would require smaller transport distances and could rely on gravity as the main driving force. Smaller transport distances are permissible because the Wernecke Supergroup had been previously deformed during the Racklan orogeny. This deformational event would allow all units of the Wernecke Supergroup to occupy the same crustal level and, upon exhumation, to be exposed at the same erosional surface, much as they are today. Therefore, emplacement of BPRI clasts to positions alongside all units of the Wernecke Supergroup could occur with little vertical displacement.

To accommodate these observations and constraints, a modified version of the tectonic model of Furlanetto *et al.* (2009b) is presented. In the Furlanetto *et al.* (2009b) model, the BPRI were part of an offshore terrane at ~1.71 Ga. Our geochemical analyses of the BPRI, and the petrologic findings of Peters and Thorkelson (this volume), indicate that the igneous megaclasts were derived from a mature volcanic arc. This igneous environment is consistent with the proposed model for the emplacement of the BPRI, because there are numerous modern examples of arc terranes being obducted onto continental cratons such as the Spong arc in the Ladahk-Zanskar Himalaya (Cornfield *et al.* 2001), the Semail supra-subduction zone ophiolite of the Oman Mountains (Shervais, 2001), and the ophiolitic nappe in New Caledonia (Aitchison *et al.*, 1995). It is also possible that the volcanic arc was built on the leading edge of a larger landmass or continent that collided with, and overrode, northwestern North America.

This model is illustrated in Figure 13, which depicts the genesis of the BPRI in an offshore arc assemblage at 1.71 Ga (Fig. 13a). After ~75 m.y., the Wernecke Supergroup began to be deposited onto ancestral North America (Fig. 13b). After sedimentation, the region was affected by contractional deformation and metamorphism, and exhumation, exposing all units of the Wernecke Supergroup (Fig. 13c). At 1.60 Ga, the volcanic arc overrode the continental margin, followed by, and possibly triggering, surges of hydrothermal fluids and the formation of Wernecke breccia. The brecciating fluids affected both the Wernecke Supergroup and the overthrust arc complex, leading to metasomatism and iron-oxide copper gold mineralization. Megaclasts of the BPRI, the Slab volcanics and other volcanic units from the nappe travelled downward in the breccia zones, some coming to rest at the level of the Wernecke Supergroup (Fig. 13d). Subsequent erosion removed the nappe and exposed BPRI-bearing breccia zones within the Wernecke Supergroup (Fig. 13e).

CONCLUSIONS

i. The BPRI consist primarily of subalkaline diorite and gabbro that are related by plagioclase and pyroxene fractionation.

ii. Clasts of the BPRI were affected by hydrothermal alteration and widespread development of iron-oxide copper gold occurrences.

iii. The BPRI and related volcanics were not derived from the Wernecke Supergroup. They were probably derived from above the Wernecke Supergroup and transported downward within Wernecke breccia to the level of the Wernecke Supergroup.

iv. The geochemical signature of the BPRI indicates that they were derived from a calc-alkaline volcanic arc that was active at ~1.71 Ga.

v. The volcanic arc was obducted over the Wernecke Supergroup after the Racklan orogeny and subsequently fragmented during hydrothermal activity of Wernecke breccia at 1.60 Ga; many clasts were dropped down to the level of the Wernecke Supergroup within zones of Wernecke breccia (Fig. 13).

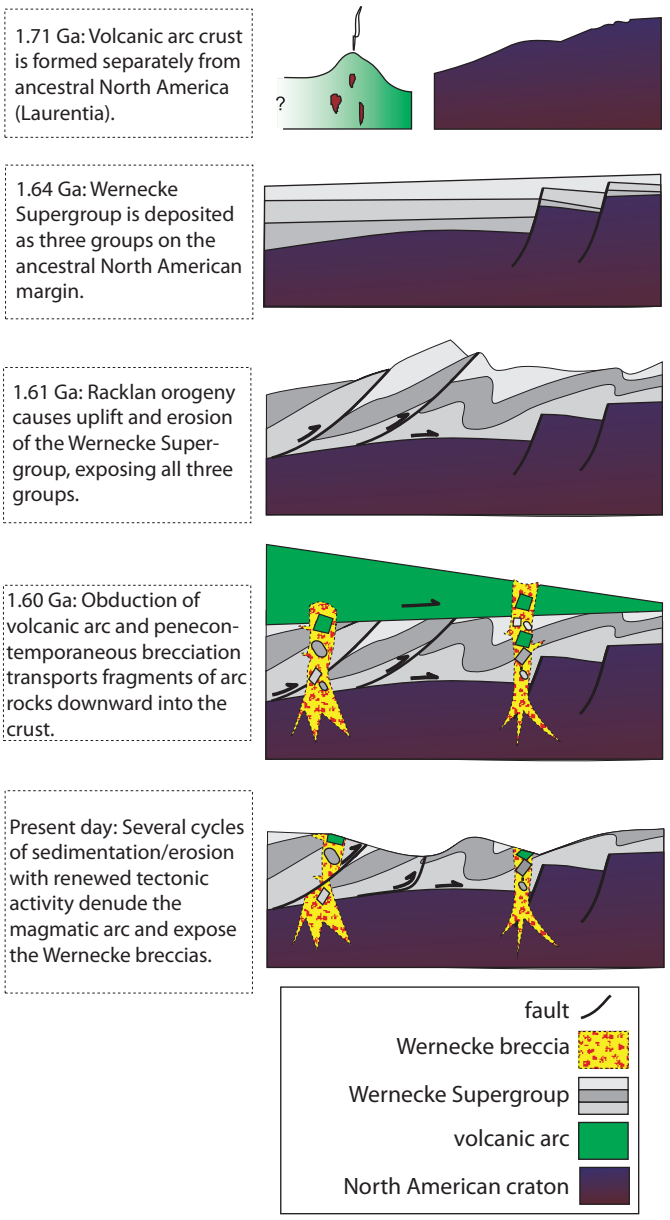

Figure 13. *Schematic history of the Bonnet Plume River intrusions, related volcanics, and the Wernecke Supergroup.*

ACKNOWLEDGEMENTS

Funding for this study was provided by the Yukon Geological Survey, the Northern Scientific Training Program, and an NSERC grant to Derek Thorkelson. The authors are grateful to Kirsti Medig and Roberta Dunlop for their assistance in the field, to Tim Peters for his assistance in the laboratory, and Elizabeth Turner for a thorough review that led to significant improvements.

REFERENCES

Aitchison, J.C., Clarke, G.L., Meffre, S. and Cluzel, D., 1995. Eocene arc-continent collision in New Caledonia and implications for regional southwest Pacific tectonic evolution. Geology, vol. 23, p. 161-164.

Basaltic Volcanism Study Project, 1981. Basaltic Volcanism on the Terrestrial Planets., Pergamon Press Inc., New York, 1286 p.

Brideau, M.-A., Thorkelson, D.J., Godin, L. and Laughton, J.R., 2002. Paleoproterozoic deformation of the Racklan Orogeny, Slats Creek (106D/16) and Fairchild Lake (106C/13) map areas, Wernecke Mountains, Yukon. *In:* Yukon Exploration and Geology 2001, D.S. Edmond, L.H. Weston and L.L. Lewis (eds.), Exploration and Geological Services Division, Yukon Region, Indian and Northern Affairs Canada, p. 65-72.

Delaney, G.D., 1981. The mid-Proterozoic Wernecke Supergroup, Wernecke Mountains, Yukon Territory. *In:* Geological Survey of Canada Paper, F.H.A. Campbell (ed.), Geological Survey of Canada, vol. 81-10, p. 1-23.

Floyd, P.A., and Winchester, J.A., 1978, Identification and discrimination of altered and metamorphosed volcanic rocks using immobile elements: Chemical Geology, vol. 21, p. 291-306.

Furlanetto, F., Thorkelson, D.J., Davis, W.J., Gibson, H.D., Rainbird, R.H. and Marshall, D.D., 2009a. Preliminary results of detrital zircon geochronology, Wernecke Supergroup, Yukon. *In:* Yukon Exploration and Geology 2008, L.H. Weston, L.R. Blackburn and L.L. Lewis (eds.), Yukon Geological Survey, p. 125 – 135.

Furlanetto, F., Thorkelson, D.J., Davis, W.J., Gibson, H.D., Rainbird, R.R. and Marshall, D.D., 2009. A new Model of Terrane Accretion in Northwestern Laurentia required by U-Pb SHRIMP Analysis of Detrital Zircons from the Paleoproterozoic Wernecke Supergroup, Wernecke Mountains, Yukon [Abstract U74A-04]. Geological Association of Canada, Joint Assembly, 24-27 May 2009, Toronto, Canada.

Gifkins, C.C., Herrmann, W. and Large, R.R., 2005. Altered volcanic rocks: a guide to description and interpretation. Centre for Ore Deposit Research, University of Tasmania, Hobart, Tasmania, 275 p.

Gill, J.B., 1981. Orogenic Andesites and Plate Tectonics. Springer-Verlag, Berlin, 390 p.

Hunt, J.A. and Thorkelson, D.J., 2007. Are mafic dykes in the Nor and Hart River areas of the Yukon correlative to the Bonnet Plume River Intrusions? Constraints from geochemistry. *In:* Yukon Exploration and Geology 2006, D.S. Emond, L.L. Lewis and L.H. Weston (eds.), Yukon Geological Survey, p. 127-137.

Irvine, G.J. and Baragar, W., 1971. A guide to the chemical classification of the common volcanic rocks. Canadian Journal of Earth Sciences, vol. 8, p. 523-584.

Laughton, J.R., 2004. The Proterozoic Slab Volcanics of Northern Yukon, Canada: Megaclasts of a Volcanic Succession in Proterozoic Wernecke Breccia, and Implications for the Evolution of Northwestern Laurentia, Earth Sciences. Simon Fraser University, Burnaby, p. 81.

Laughton, J.R., Thorkelson, D.J., Brideau, M.-A. and Hunt, J.A., 2002. Paleoproterozoic volcanism and plutonism in the Wernecke Mountains, Yukon. *In:* Yukon Exploration and Geology 2001, D.S. Emond, L.H. Weston and L.L. Lewis (eds.), Exploration and Geological Services Division, Yukon Region, Indian and Northern Affairs Canada, p. 139-145.

LeMaitre, R.W., 2002, Igneous Rocks: A Classification and Glossary of Terms. Recommendations of the International Union of Geological Sciences Subcommission on the Systematics of Igneous Rocks, Cambridge University Press, Cambridge, UK, 256 p.

Miyashiro, A., 1974. Volcanic rock series in island arcs and active continental margins. American Journal of Science, vol. 274, p. 321-355.

Norris, D.K., 1997. Geology and mineral and hydrocarbon potential of northern Yukon Territory and northwestern district of Mackenzie. Geological Survey of Canada Bulletin, vol. 422, 401 p.

Pecerillo, A. and Taylor, S.R., 1976. Geochemistry of Eocene calc-alkaline volcanic rocks from the Kastamonu area, Northern Turkey. Contributions to Mineralogy and Petrology, vol. 58, p. 63-81.

Peters, T.J. and Thorkelson, D.J., (this volume). Volcano-sedimentary megaclast in Wernecke breccia, Yukon, and its bearing on the Proterozoic evolution of northwestern Laurentia. *In:* Yukon Exploration and Geology 2010, K.E. MacFarlane, L.H. Weston and C. Relf (eds.), Yukon Geological Survey.

Rollinson, 1993. Using Geochemical Data: Evaluation, Presentation, Interpretation. Longman Scientific and Technical, London, UK, 352 p.

Ross, P. and Bédard, J.H., 2009. Magmatic affinity of modern and ancient subalkaline volcanic rocks determined from trace-element discriminant diagrams. Canadian Journal of Earth Sciences, vol. 46, p. 823-839.

Shervais, J.W., 1982. Ti-V plots and the petrogenesis of modern and ophiolitic lavas. Earth and Planetary Science Letters, vol. 59, p. 101-118.

Shervais, J.W., 2001. Birth, death, and resurrection: The life cycle of suprasubduction zone ophiolites. Geochemistry Geophysics Geosystems, vol. 2, no. 1, 1010, 45 p. doi:10.1029/2000GC000080

Thorkelson, D.J., 2000. Geology and Mineral Occurrences of the Slats Creek, Fairchild Lake and "Dolores Creek" Areas, Wernecke Mountains (106D/16, 106C/13, 106C/14), Yukon Territory. Exploration and Geological Services Division, Yukon, Indian and Northern Affairs Canada, Bulletin 10, 73 p.

Thorkelson, D.J. and Wallace, C.W., 1998a. Geological map of Slats Creek area, Wernecke Mountains, Yukon (106D/16). Exploration and Geological Services Division, Yukon, Indian and Northern Affairs Canada, Geoscience Map 1998-9, scale 1:50 000.

Thorkelson, D.J. and Wallace, C.W., 1998b. Geological map of Fairchild Lake area, Wernecke Mountains, Yukon (106C/13). Exploration and Geological Services Division, Yukon, Indian and Northern Affairs Canada, Geoscience Map 1998-10, scale 1:50 000.

Thorkelson, D.J. and Wallace, C.W., 1998c. Geological map of Dolores Creek area, Wernecke Mountains, Yukon (106C/14). Exploration and Geological Services Division, Yukon, Indian and Northern Affairs Canada, Geoscience Map 1998-11, scale 1:50 000.

Thorkelson, D.J., Mortensen, J.K., Creaser, R.A., Davidson, G.J. and Abbott, J.G., 2001a. Early Proterozoic magmatism in Yukon, Canada: constraints on the evolution of northwestern Laurentia. Canadian Journal of Earth Sciences, vol. 38, p. 1479 – 1494.

Thorkelson, D.J., Mortensen, J.K., Davidson, G.J., Creaser, R.A., Perez, W.A. and Abbott, J.G., 2001b. Early Mesoproterozoic intrusive breccias in Yukon, Canada: the role of hydrothermal systems in reconstructions of North America and Australia. Precambrian Research, vol. 111, p. 31-55.

Winchester, J.A. and Floyd, P.A., 1977. Geochemical discrimination of different magma series and their differentiation products using immobile elements. Chemical Geology, vol. 20, p. 325-343.

Wood, D.A., 1980. The Application of a Th-Hf-Ta diagram to problems of tectonomagmatic classification and to establishing the nature of crustal contamination of basaltic lavas of the British Tertiary Volcanic Province: Earth and Planetary Science Letters, vol. 50, issue 1, p. 11-30.

Yukon MINFILE, 2010. Yukon MINFILE – A database of mineral occurrences. Yukon Geological Survey, <http://www.geology.gov.yk.ca/databases_gis.html>, [accessed November 2010]